

# Renormalons and the Top quark mass measurement

Paolo Nason

*Work done in collaboration with  
Silvia Ferrario Ravasio and Carlo Oleari*

CERN and INFN, sez. di Milano Bicocca

LHC TOP WG, CERN, November 20 2018

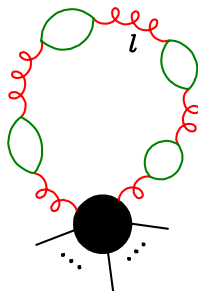
# Outline

- ▶ A reminder on renormalons
- ▶ What we computed and why
- ▶ Some results
- ▶ Conclusions
- ▶ Prospects

# ABC of I.R. Renormalons

All-orders contributions to QCD amplitude of the form

$$\begin{aligned}\int_0^m dk^P \alpha_s(k^2) &= \int_0^m dk^P \frac{\alpha_s(m^2)}{1 + b_0 \alpha_s(m^2) \log \frac{k^2}{m^2}} \\ &= \alpha_s(m^2) \sum_{n=0}^{\infty} (2b_0 \alpha_s(m^2))^n \underbrace{\int_0^m dk^P \log^n \frac{m}{k}}_{p^n n!}.\end{aligned}$$



Asymptotic expansion.

Arises from **all order leading-logarithmic corrections** induced by the **coupling constant renormalization**.

In **QED** these are the **sum of all photon polarization corrections**.

In QCD not quite so ... **but the substance is the same**.

- Minimal term at  $n_{\min} \approx \frac{1}{2pb_0\alpha_s(m^2)}$ .
- Size of minimal term:  $m^p \alpha_s(m^2) \sqrt{2\pi n_{\min}} e^{-n_{\min}} \approx \Lambda_{\text{QCD}}^p$ .
- Typical scale dominating at order  $\alpha_s^{n+1}$ :  $m \exp(-np)$ .

Notice: parametric form of the minimal term consistent with the presence of the Landau pole at  $k = m \exp(\frac{1}{2\alpha_s(m^2)b_0}) = \Lambda_{\text{QCD}}$ :

$$\int_0^m dk^p \alpha_s(k^2) \quad (1)$$

become ambiguous when  $\alpha_s(k^2) \approx 1$ , i.e.  $k \approx \Lambda_{\text{QCD}}$ , leading to a  $\Lambda_{\text{QCD}}^p$  ambiguity.

# The large $b_0$ approximation

In QED, the diagrams leading to renormalons are the polarization insertions in photon propagators.

An often used approximation to estimate renormalon contributions on QCD is by considering only polarization insertions into the gluon propagator due to light quarks, leading to  $b_0^{(n_f)} = -\frac{n_f T_f}{3\pi}$  colour factors. At the end of the calculation, one replaces the  $b_0^{(n_f)}$  with the true QCD  $b_0$ :

$$-\frac{n_f}{3\pi} \rightarrow \frac{11C_A - 4n_f T_f}{12\pi}.$$

This is the so called large- $b_0$  approximation.

## Abstract:

The resummed Drell-Yan cross section in the double-logarithmic approximation suffers from infrared renormalons. Their presence was interpreted as an indication for non-perturbative corrections of order  $\Lambda_{\text{QCD}}/(Q(1-z))$ . We find that, once soft gluon emission is accurately taken into account, the leading renormalon divergence is cancelled by higher-order perturbative contributions in the exponent of the resummed cross section.

Their calculation: large  $b_0$  approximation:

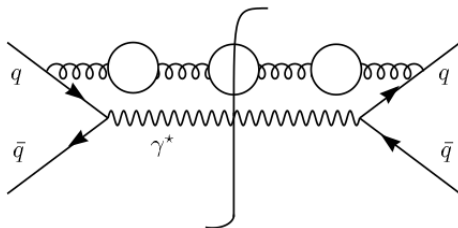
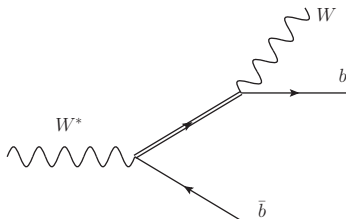


Figure 1:  $\alpha_s^4$ -contribution to the partonic Drell-Yan cross section.  $\gamma^*$  represents a photon with invariant mass  $Q^2$  that splits into a lepton pair.

# Top mass measurements

- ▶ Linear (i.e.  $p = 1$ ) renormalons may affect top mass measurements at order  $\Lambda$  (near the present experimental accuracy). Until now, only the **top pole mass renormalons** has received some attention.
- ▶ Several other sources of linear renormalons come into play in top mass measurements (for example, from jet definition). What is their structure, and what is their interplay with the pole mass renormalon?
- ▶ Are there “privileged” (i.e. no  $p = 1$  renormalons) observables?

We consider a simplified production framework  $W^* \rightarrow W t \bar{b}$ :

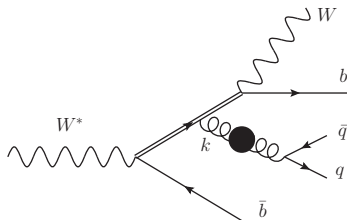
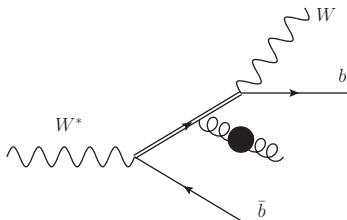
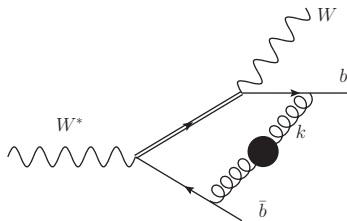
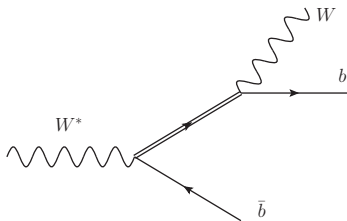


(i.e. no incoming hadrons for now), and a massless  $b$ . However:

- The finite width of the top is accounted for;
- We can consider any IR safe final state observables.



# Diagrams up to leading $N_f$ one gluon correction



$$\text{Gluon self-energy blob} = \text{Gluon self-energy} + \text{Gluon self-energy with quark loop}$$

The equation shows the decomposition of a gluon self-energy correction (represented by a curly line, a black blob, and another curly line) into a tree-level gluon self-energy (two curly lines) and a one-loop gluon self-energy (two curly lines, a white circle with arrows, and another curly line) followed by a black blob.

# All-order result

Introducing the notation

- ▶  $\Phi_b$ , phase space for  $Wb\bar{b}$ ;
- ▶  $\Phi_g$ , phase space for  $Wb\bar{b}g^*$ , where  $g^*$  is a massive gluon with mass  $\lambda$ ,
- ▶  $\Phi_{q\bar{q}}$ , phase space for  $Wb\bar{b}q\bar{q}$

the all-order result can be expressed in terms of

- ▶  $\sigma_b(\Phi_b)$ , the differential cross section for the Born process;
- ▶  $\sigma_v(\lambda, \Phi_b)$ , the virtual correction to the Born process due to the exchange of a gluon of mass  $\lambda$ ;
- ▶ The real cross section  $\sigma_{g^*}(\lambda, \Phi_{g^*})$ , obtained by adding one massive gluon to the Born final state;
- ▶ The real cross section  $\sigma_{q\bar{q}}(\Phi_{q\bar{q}})$ , obtained by adding a  $q\bar{q}$  pair, produced by a massless gluon, to the Born final state;

## All-order result

Consider a (IR safe) final state observable  $O$ . Define:

$$N^{(0)} = \left[ \int d\Phi_b \sigma_b \right]^{-1}, \quad \langle O \rangle_b = N^{(0)} \int d\Phi_b \sigma_b(\Phi_b) O(\Phi_b),$$

$$\tilde{V}(\lambda) = N^{(0)} \int d\Phi_b \sigma_v^{(1)}(\lambda, \Phi_b) [O(\Phi_b) - \langle O \rangle_b],$$

$$\tilde{R}(\lambda) = N^{(0)} \int d\Phi_{g^*} \sigma_{g^*}^{(1)}(\lambda, \Phi_{g^*}) [O(\Phi_{g^*}) - \langle O \rangle_b],$$

$$\tilde{\Delta}(\lambda) = N^{(0)} \frac{3\lambda^2}{2\alpha_s T_F} \int d\Phi_{q\bar{q}} \delta(\lambda^2 - k_{q\bar{q}}^2) \sigma_{q\bar{q}}^{(2)}(\Phi_{q\bar{q}}) \times [O(\Phi_{q\bar{q}}) - O(\Phi_{g^*})]$$

$\langle O \rangle_b + \tilde{V}(\lambda) + \tilde{R}(\lambda)$  is the average value of  $O$  in a theory with a massive gluon with mass  $\lambda$ , accurate to order  $\alpha_s$ .

Notice:  $\tilde{V}(\lambda) + \tilde{R}(\lambda)$  has a finite limit for  $\lambda \rightarrow 0$ , while each contribution is log divergent.

defining  $\tilde{T}(\lambda) \equiv \tilde{V}(\lambda) + \tilde{R}(\lambda) + \tilde{\Delta}(\lambda)$ , our final result is

$$\langle O \rangle = \langle O \rangle_b + \frac{3\pi}{\alpha_s T_F} \int_0^\infty \frac{d\lambda}{\pi} \frac{d}{d\lambda} [\tilde{T}(\lambda)] \operatorname{atan} \left( \frac{\alpha_s \pi b_0}{1 + \alpha_s b_0 \log \frac{\lambda^2}{\tilde{\mu}^2}} \right) \quad (2)$$

where  $\tilde{\mu} \equiv \mu \exp(5/6)$ .

This has the same renormalon structure of the example we considered at the beginning. Now the `atan` function has an unphysical discontinuity near the Landau pole

$$\lambda^2 = \tilde{\mu}^2 \exp \left[ \frac{1}{\alpha_s(\mu) b_0} \right] = \Lambda_{\text{QCD}}^2 \exp(5/3). \quad (3)$$

If we thus have:

$$\tilde{T}(\lambda) = a + b\lambda + \mathcal{O}(\lambda^2) \quad (4)$$

the integration has an ambiguity of order  $b\Lambda_{\text{QCD}}$ , i.e. a Linear Renormalon.

- ▶ In order to get our results, we need  $\lim_{\lambda \rightarrow \infty} \tilde{T}(\lambda) = 0$ .  
This happens if we use the **Pole Mass Scheme** for  $m_t$ .
- ▶ The need to include the  $\Delta$  term has a long story:
  - ▶ Seymour, P.N. 1995, I.R. renormalons in  $e^+e^-$  event shapes.
  - ▶ Dokshitzer, Lucenti, Marchesini, Salam, 1997-1998 Milan factor
- ▶ We compute  $T(\lambda)$  numerically. The  $\lambda \rightarrow 0$  limit implies the cancellation of two large logs in  $V$  and  $R$ . However, the precise value at  $\lambda = 0$  can also be computed directly by standard means (which we do).

## Changing the mass scheme

The relation of the pole mass as a function of the  $\overline{\text{MS}}$  mass in the large  $N_F$  approximation is well known ([Beneke, 1999](#))

$$\begin{aligned}m &= \bar{m}[1 + R_f(\alpha_s, \mu, \bar{m}) + R_d(\alpha_s, \mu, \bar{m})], \\R_f &= -\frac{3\pi}{\alpha_s T_F} \int_0^\infty \frac{d\lambda}{\pi} \frac{dr_f(\lambda)}{d\lambda} \operatorname{atan} \frac{-\alpha_s \pi b_0}{1 + \alpha_s b_0 \log \frac{\lambda^2}{\bar{\mu}^2}} \\r_f(\lambda) &= -\alpha_s \frac{C_F}{2} \frac{\lambda}{m}.\end{aligned}\tag{5}$$

We can easily convert our results to the  $\overline{\text{MS}}$  scheme:

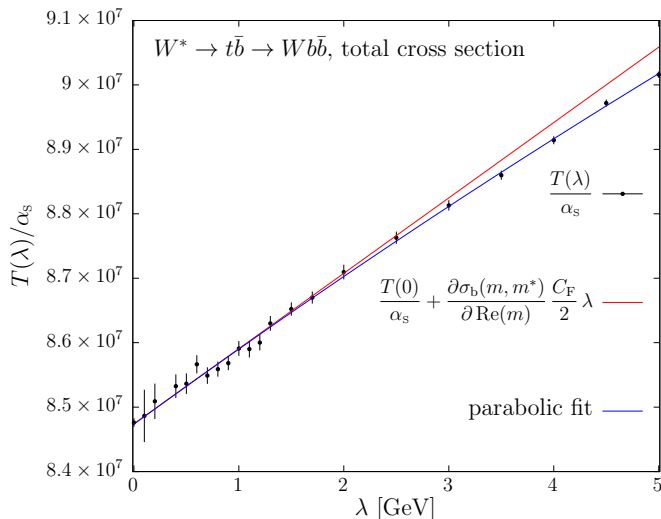
$$\langle O \rangle_b(m, m^*) = \langle O \rangle_b(\bar{m}, \bar{m}^*) + \left\{ \frac{\partial \langle O \rangle_b(\bar{m}, \bar{m}^*)}{\partial \bar{m}} (m - \bar{m}) + \text{cc} \right\}$$

For the leading renormalon this amounts to

$$\tilde{T}(\lambda) \rightarrow \tilde{T}(\lambda) - \frac{\partial \langle O \rangle_b(\bar{m}, \bar{m}^*)}{\partial \operatorname{Re}(\bar{m})} \frac{C_F \alpha_s}{2} \lambda + \mathcal{O}(\lambda^2).$$

## SELECTED RESULTS

# Total cross section



No linear renormalon in  $\overline{\text{MS}}$  scheme!

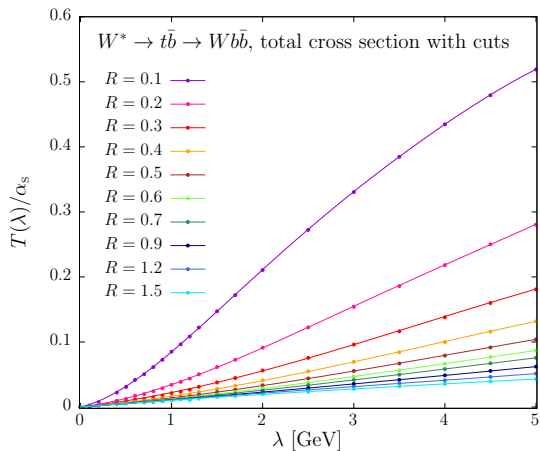


# Total cross section

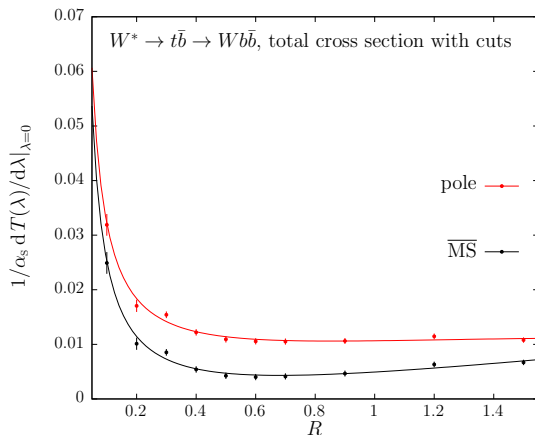
- For  $k < \Gamma$ : no renormalon in the physics! The top finite width screens the soft sensitivity of the cross section.  
The renormalon is there only if it is present in the mass counterterm; thus, it is not there in the  $\overline{\text{MS}}$  scheme.
- What about  $k \gg \Gamma$ ?  
This is the narrow width limit: the cross section factorizes into a production cross section and a partial width.  
The former has no physical renormalons for obvious reasons.  
The latter does not have them either (not obvious at all? known fact from  $B$  decay theory)

So, the mass from the total  $\sigma$  is free of linear power corrections

# Total cross section with cuts

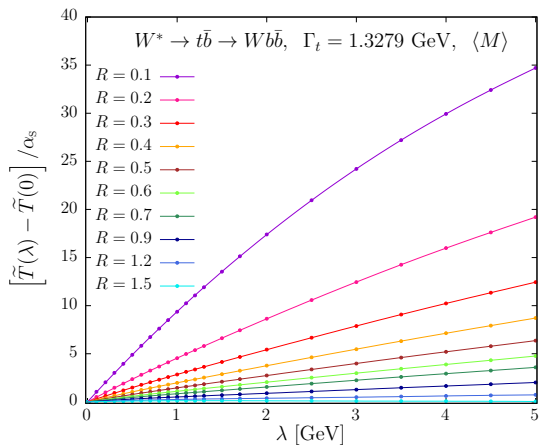


# Total cross section with cuts

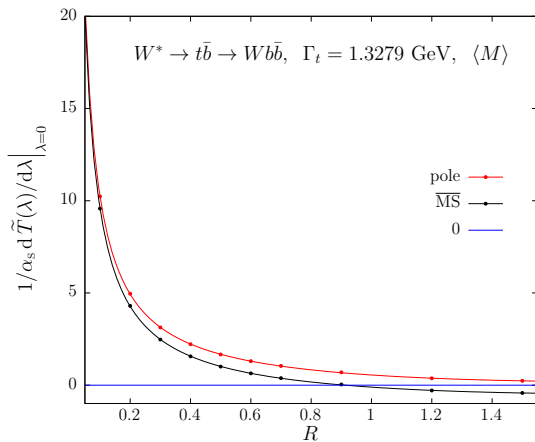


The requirement of a  $b$  jet spoils this conclusion!

# Reconstructed top mass



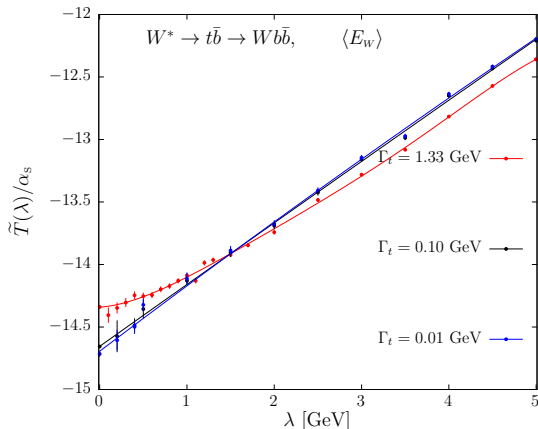
# Reconstructed top mass



For large radii,  $m_{\text{pole}}$  is better!

# Leptonic Observables

Choose as mass sensitive observable the average  $E_W$ .



For  $k \gg \Gamma$ , the slope is roughly 0.45. The  $\overline{\text{MS}}$  conversion would add  $-0.067$ .

It seems that physical linear renormalons are present also in leptonic observables.

But, for  $k \ll \Gamma$ , the slope of  $T(k)$  decreases, approaching 0.067!  
So, the top finite width screens the linear renormalons!

Is this an exact statement?

YES! (we can prove it ...)

# Perturbative expansion

Besides computing the effect of the linear renormalon, we can compute also the **exact** (in the large  $b_0$  limit) perturbative corrections order-by-order in perturbation theory, and explicitly check how they are affected by IR renormalons.



|     | $\sigma/\sigma_b^{\text{nocuts}}(m)$ |                            |                               |                            |
|-----|--------------------------------------|----------------------------|-------------------------------|----------------------------|
|     | pole scheme                          |                            | $\overline{\text{MS}}$ scheme |                            |
| $i$ | $c_i$                                | $c_i \alpha_s^i$           | $c_i$                         | $c_i \alpha_s^i$           |
| 0   | 1.00000000                           | 1.00000000                 | 0.86841331                    | 0.8684133                  |
| 1   | $5.003 (0) \times 10^{-1}$           | $5.411 (0) \times 10^{-2}$ | $1.480 (0) \times 10^0$       | $1.601 (0) \times 10^{-1}$ |
| 2   | $-6.20 (2) \times 10^{-1}$           | $-7.25 (2) \times 10^{-3}$ | $4.42 (2) \times 10^{-1}$     | $5.17 (2) \times 10^{-3}$  |
| 3   | $-3.03 (2) \times 10^0$              | $-3.83 (3) \times 10^{-3}$ | $6.4 (2) \times 10^{-1}$      | $8.1 (3) \times 10^{-4}$   |
| 4   | $-1.25 (2) \times 10^1$              | $-1.70 (3) \times 10^{-3}$ | $0 (2) \times 10^{-2}$        | $0 (3) \times 10^{-6}$     |
| 5   | $-6.4 (2) \times 10^1$               | $-9.4 (3) \times 10^{-4}$  | $1 (2) \times 10^{-1}$        | $1 (3) \times 10^{-5}$     |
| 6   | $-3.9 (1) \times 10^2$               | $-6.2 (2) \times 10^{-4}$  | $0 (1) \times 10^0$           | $0 (2) \times 10^{-6}$     |
| 7   | $-2.9 (1) \times 10^3$               | $-5.0 (2) \times 10^{-4}$  | $0 (1) \times 10^1$           | $0 (2) \times 10^{-6}$     |
| 8   | $-2.5 (1) \times 10^4$               | $-4.6 (2) \times 10^{-4}$  | $0 (1) \times 10^2$           | $0 (2) \times 10^{-6}$     |
| 9   | $-2.4 (1) \times 10^5$               | $-4.9 (2) \times 10^{-4}$  | $0 (1) \times 10^3$           | $0 (2) \times 10^{-6}$     |
| 10  | $-2.6 (1) \times 10^6$               | $-5.8 (2) \times 10^{-4}$  | $0 (1) \times 10^4$           | $-1 (2) \times 10^{-6}$    |

**Table 3:** Coefficients of the  $\alpha_s$  expansion (8.4) of the inclusive cross section to all orders, computed in the large- $b_0$  approximation, normalized to the total Born cross section computed in the pole-mass scheme. The errors reported in parenthesis are due to the uncertainty on the linear coefficient of the fit (i.e.  $p_1$  in eq. (8.3)).

| $\sigma/\sigma_b^{\text{nocuts}}(m) \quad R = 0.1$ |                            |                               | $\sigma/\sigma_b^{\text{nocuts}}(m) \quad R = 0.5$ |                            |                               |
|----------------------------------------------------|----------------------------|-------------------------------|----------------------------------------------------|----------------------------|-------------------------------|
|                                                    | pole scheme                | $\overline{\text{MS}}$ scheme |                                                    | pole scheme                | $\overline{\text{MS}}$ scheme |
| $i$                                                | $c_i \alpha_s^i$           | $c_i \alpha_s^i$              | $i$                                                | $c_i \alpha_s^i$           | $c_i \alpha_s^i$              |
| 0                                                  | 0.9985836                  | 0.8666708                     | 0                                                  | 0.9783310                  | 0.8511828                     |
| 1                                                  | $-7.953(0) \times 10^{-2}$ | $2.650(0) \times 10^{-2}$     | 1                                                  | $-4.992(0) \times 10^{-3}$ | $9.705(0) \times 10^{-2}$     |
| 2                                                  | $-7.22(2) \times 10^{-2}$  | $-5.98(2) \times 10^{-2}$     | 2                                                  | $-2.966(5) \times 10^{-2}$ | $-1.779(5) \times 10^{-2}$    |
| 3                                                  | $-3.71(2) \times 10^{-2}$  | $-3.24(2) \times 10^{-2}$     | 3                                                  | $-1.267(6) \times 10^{-2}$ | $-8.22(6) \times 10^{-3}$     |
| 4                                                  | $-1.97(2) \times 10^{-2}$  | $-1.80(2) \times 10^{-2}$     | 4                                                  | $-5.37(6) \times 10^{-3}$  | $-3.73(6) \times 10^{-3}$     |
| 5                                                  | $-1.13(2) \times 10^{-2}$  | $-1.04(2) \times 10^{-2}$     | 5                                                  | $-2.58(5) \times 10^{-3}$  | $-1.66(5) \times 10^{-3}$     |
| 6                                                  | $-7.0(2) \times 10^{-3}$   | $-6.4(2) \times 10^{-3}$      | 6                                                  | $-1.44(4) \times 10^{-3}$  | $-8.5(4) \times 10^{-4}$      |
| 7                                                  | $-4.8(1) \times 10^{-3}$   | $-4.3(1) \times 10^{-3}$      | 7                                                  | $-9.8(4) \times 10^{-4}$   | $-5.0(4) \times 10^{-4}$      |
| 8                                                  | $-3.6(1) \times 10^{-3}$   | $-3.1(1) \times 10^{-3}$      | 8                                                  | $-8.1(4) \times 10^{-4}$   | $-3.7(4) \times 10^{-4}$      |
| 9                                                  | $-3.1(1) \times 10^{-3}$   | $-2.7(1) \times 10^{-3}$      | 9                                                  | $-8.0(4) \times 10^{-4}$   | $-3.4(4) \times 10^{-4}$      |
| 10                                                 | $-3.2(2) \times 10^{-3}$   | $-2.6(2) \times 10^{-3}$      | 10                                                 | $-9.2(5) \times 10^{-4}$   | $-3.7(5) \times 10^{-4}$      |

**Table 4:** Coefficients  $c_i$  of the  $\alpha_s$  expansion (8.4) of the cross section with cuts, to all orders, computed in the large- $b_0$  approximation, normalized to the total Born cross section computed in the pole-mass scheme, for two different values of the jet radius ( $R = 0.1$  in the left pane and  $R = 0.5$  in the right one). The errors reported in parenthesis are due to the uncertainty on the linear coefficient of the fit (i.e.  $p_1$  in eq. (8.3)).

| $i$ | $R = 0.1$                 |                           | $R = 0.5$                 |                           | $R = 1.5$                 |                          |
|-----|---------------------------|---------------------------|---------------------------|---------------------------|---------------------------|--------------------------|
|     | pole                      | $\overline{\text{MS}}$    | pole                      | $\overline{\text{MS}}$    | pole                      | $\overline{\text{MS}}$   |
| 0   | 172.8280                  | 163.0146                  | 172.8201                  | 163.0040                  | 172.7533                  | 162.9244                 |
| 1   | $-7.597(0) \times 10^0$   | $2.163(0) \times 10^{-1}$ | $-2.785(0) \times 10^0$   | $5.030(0) \times 10^0$    | $4.446(0) \times 10^{-1}$ | $8.268(0) \times 10^0$   |
| 2   | $-4.136(2) \times 10^0$   | $-2.852(2) \times 10^0$   | $-1.255(1) \times 10^0$   | $2.9(1) \times 10^{-2}$   | $1.029(8) \times 10^{-1}$ | $1.387(1) \times 10^0$   |
| 3   | $-2.397(2) \times 10^0$   | $-1.973(2) \times 10^0$   | $-5.96(2) \times 10^{-1}$ | $-1.72(2) \times 10^{-1}$ | $1.4(1) \times 10^{-2}$   | $4.38(1) \times 10^{-1}$ |
| 4   | $-1.505(2) \times 10^0$   | $-1.337(2) \times 10^0$   | $-3.13(2) \times 10^{-1}$ | $-1.44(2) \times 10^{-1}$ | $-6(1) \times 10^{-3}$    | $1.63(1) \times 10^{-1}$ |
| 5   | $-1.038(2) \times 10^0$   | $-9.50(2) \times 10^{-1}$ | $-1.88(2) \times 10^{-1}$ | $-1.00(2) \times 10^{-2}$ | $-9.7(9) \times 10^{-3}$  | $7.86(9) \times 10^{-2}$ |
| 6   | $-7.94(2) \times 10^{-1}$ | $-7.35(2) \times 10^{-1}$ | $-1.33(1) \times 10^{-1}$ | $-7.3(1) \times 10^{-2}$  | $-1.05(8) \times 10^{-2}$ | $4.89(8) \times 10^{-2}$ |
| 7   | $-6.79(2) \times 10^{-1}$ | $-6.33(2) \times 10^{-1}$ | $-1.09(1) \times 10^{-1}$ | $-6.3(1) \times 10^{-2}$  | $-1.12(7) \times 10^{-2}$ | $3.53(7) \times 10^{-2}$ |
| 8   | $-6.51(2) \times 10^{-1}$ | $-6.08(2) \times 10^{-1}$ | $-1.04(1) \times 10^{-1}$ | $-6.1(1) \times 10^{-2}$  | $-1.25(7) \times 10^{-2}$ | $3.08(7) \times 10^{-2}$ |
| 9   | $-6.99(2) \times 10^{-1}$ | $-6.54(2) \times 10^{-1}$ | $-1.12(1) \times 10^{-1}$ | $-6.7(1) \times 10^{-2}$  | $-1.47(7) \times 10^{-2}$ | $3.09(7) \times 10^{-2}$ |
| 10  | $-8.37(2) \times 10^{-1}$ | $-7.83(2) \times 10^{-1}$ | $-1.35(1) \times 10^{-1}$ | $-8.1(1) \times 10^{-2}$  | $-1.85(9) \times 10^{-2}$ | $3.57(9) \times 10^{-2}$ |

**Table 5:** Values of the  $c_i \alpha_s^i$  terms of the perturbative expansion for the average value of the reconstructed-top mass, defined in eq. (8.5), for three different jet radii, in the pole-mass and  $\overline{\text{MS}}$ -mass scheme. The errors reported in parenthesis are due to the uncertainty on the linear coefficient of the fit (i.e.  $p_1$  in eq. (8.3)).

|     | $\langle E_W \rangle$   |                           |                               |                            |
|-----|-------------------------|---------------------------|-------------------------------|----------------------------|
|     | pole scheme             |                           | $\overline{\text{MS}}$ scheme |                            |
| $i$ | $c_i$                   | $c_i \alpha_S^i$          | $c_i$                         | $c_i \alpha_S^i$           |
| 0   | 121.5818                | 121.5818                  | 120.8654                      | 120.8654                   |
| 1   | $-1.435(0) \times 10^1$ | $-1.552(0) \times 10^0$   | $-7.192(0) \times 10^0$       | $-7.779(0) \times 10^{-1}$ |
| 2   | $-4.97(4) \times 10^1$  | $-5.82(4) \times 10^{-1}$ | $-3.88(4) \times 10^1$        | $-4.54(4) \times 10^{-1}$  |
| 3   | $-1.79(5) \times 10^2$  | $-2.26(6) \times 10^{-1}$ | $-1.45(5) \times 10^2$        | $-1.84(6) \times 10^{-1}$  |
| 4   | $-6.9(4) \times 10^2$   | $-9.4(6) \times 10^{-2}$  | $-5.7(4) \times 10^2$         | $-7.8(6) \times 10^{-2}$   |
| 5   | $-2.9(3) \times 10^3$   | $-4.4(5) \times 10^{-2}$  | $-2.4(3) \times 10^3$         | $-3.5(5) \times 10^{-2}$   |
| 6   | $-1.4(3) \times 10^4$   | $-2.2(4) \times 10^{-2}$  | $-1.0(3) \times 10^4$         | $-1.7(4) \times 10^{-2}$   |
| 7   | $-8(2) \times 10^4$     | $-1.3(4) \times 10^{-2}$  | $-5(2) \times 10^4$           | $-8(4) \times 10^{-3}$     |
| 8   | $-5(2) \times 10^5$     | $-9(4) \times 10^{-3}$    | $-2(2) \times 10^5$           | $-4(4) \times 10^{-3}$     |
| 9   | $-3(2) \times 10^6$     | $-7(4) \times 10^{-3}$    | $-1(2) \times 10^6$           | $-2(4) \times 10^{-3}$     |
| 10  | $-3(2) \times 10^7$     | $-6(5) \times 10^{-3}$    | $0(2) \times 10^6$            | $-1(5) \times 10^{-4}$     |
| 11  | $-3(3) \times 10^8$     | $-7(6) \times 10^{-3}$    | $0(3) \times 10^6$            | $0(6) \times 10^{-5}$      |
| 12  | $-4(3) \times 10^9$     | $-9(9) \times 10^{-3}$    | $0(3) \times 10^8$            | $1(9) \times 10^{-3}$      |

**Table 6:** Coefficients of the perturbative expansion (8.6) of the average  $W$ -boson energy in the pole and  $\overline{\text{MS}}$ -mass schemes. The errors reported in parenthesis are due to the uncertainty on the linear coefficient of the fit (i.e.  $p_1$  in eq. (8.3)).

# Conclusions

- ▶ This work is addressing theoretical questions having to do with the high-order perturbative structure, in its relation to power corrections.
- ▶ Many simplifying assumptions were made; some of them may be removed in the future.
- ▶ In spite of the simplifying assumption, several results have implications even for current measurements:
  - ▶ Although there are good reasons to believe that the total cross section is not affected by linear renormalons, as soon as we introduce acceptance cuts, linear corrections, especially due to jets, do appear.
  - ▶ For observables that do not depend upon jets, the finite width at the top seems to screen linear renormalon effects. Leptonic observables could benefit from this. In practice, however, this feature does not help at the moment, since it requires very high order calculations.
  - ▶ Leptonic observables are also affected by linear renormalons, unless one goes at very high order in their perturbative calculation.

There are several directions in which this work can be extended.

- ▶ Study observables where jets are calibrated. See if linear renormalons are reduced, and to what extent.
- ▶ Does jet trimming reduce linear renormalon effects?
- ▶ In general, are there “better” observables from this point of view?